Influence of Ca^{2+} on Force Redevelopment Kinetics in Skinned Rat Myocardium

William O. Hancock,* Donald A. Martyn,* Lee L. Huntsman,* and Albert M. Gordon‡
*Center for Bioengineering and ‡Department of Physiology and Biophysics University of Washington, Seattle, Washington 98195 USA

ABSTRACT The influence of Ca^{2+} on isometric force kinetics was studied in skinned rat ventricular trabeculae by measuring the kinetics of force redevelopment after a transient decrease in force. Two protocols were employed to rapidly detach cycling myosin cross-bridges: a large-amplitude muscle length ramp followed by a restretch back to the original length or a 4% segment length step. During the recovery of force, the length of the central region of the muscle was controlled by using a segment marker technique and software feedback control. Tension redevelopment was fit by a rising exponential governed by the rate constant k_{tr} for the ramp/restretch protocol and k_{step} for the step protocol. k_{tr} and k_{step} averaged 7.06 s^{-1} and 15.7 s^{-1}, respectively, at 15°C; neither k_{tr} nor k_{step} increased with the level of Ca^{2+} activation. Similar results were found at submaximum Ca^{2+} levels when sarcomere length control by laser diffraction was used. The lack of activation dependence of k_{tr} contrasts with results from fast skeletal fibers, in which k_{tr} varies 10-fold from low to high activation levels, and suggests that Ca^{2+} does not modulate the kinetics of cross-bridge attachment or detachment in mammalian cardiac muscle.

INTRODUCTION

Cardiac muscle contraction is triggered by the binding of Ca^{2+} to troponin C (TnC), the Ca^{2+}-binding subunit of the troponin regulatory complex, which causes a structural change in the thin filament that leads to enhanced actomyosin interaction. Although it is established that an increase in Ca^{2+} binding leads to force generation and muscle shortening, neither the steps following Ca^{2+} binding nor the role that Ca^{2+} plays in turning on myocardial contraction is well understood. The regulation of contraction by Ca^{2+} has historically been explained by the steric blocking model (Huxley, 1973; Parry and Squire, 1973), which holds that the interaction of myosin with actin is inhibited in the absence of Ca^{2+} by the thin filament protein tropomyosin and that Ca^{2+} binding to the thin filament relieves this inhibition, resulting in force generation and muscle shortening. This model is supported by structural studies using both x-ray diffraction (Huxley, 1973; Kress et al., 1986) and, more recently, three-dimensional electron microscopic reconstruction of the thin filament (Lehman et al., 1994), which suggest that Ca^{2+} binding causes tropomyosin to shift its position relative to actin, exposing myosin-binding sites. However, the model is not able to account for all results, and other models do exist.

The kinetics of cross-bridge attachment and detachment can be measured in muscle fibers by studying the redevelopment of force after rapid cross-bridge detachment (Brenner and Eisenberg, 1986). It has been shown that if a skeletal fiber is allowed to shorten for a time under zero load and then is rapidly stretched back to its original length to detach any cycling cross-bridges, the result is that force and stiffness fall to low levels. The subsequent redevelopment of force after restretch is thought to reflect the kinetics of cross-bridge attachment and detachment and can be described by a rising exponential function governed by the tension redevelopment rate constant, k_{tr}. With this technique, changes in cross-bridge kinetics under various conditions can be resolved by measuring differences in k_{tr}.

In fast skeletal fibers, k_{tr} has been found to vary nearly 10-fold from submaximum to maximum Ca^{2+} activation levels, which has led to a model of contractile regulation in which the number of myosin cross-bridges that interact with actin is constant, and instead Ca^{2+} modulates the kinetics of transitions between the non-force-producing and force-producing states within the actomyosin cross-bridge cycle (Brenner, 1988). In this model, the rate of cross-bridge detachment remains constant, but the cross-bridge attachment rate constant increases with $[Ca^{2+}]$, leading to greater attachment and hence force at elevated $[Ca^{2+}]$. This model is able to account for many facets of contractile regulation in skeletal muscle and presents an alternative paradigm to the steric blocking model of Ca^{2+} regulation, although the two models are not mutually exclusive. However, although these two paradigms have been applied to skeletal muscle, their applicability to cardiac muscle is not known. To distinguish between these two models of contractile regulation and to provide experimental data from which to formulate other models of contractile regulation, it is necessary to determine the influence of Ca^{2+} on force redevelopment kinetics in cardiac muscle.

We previously studied the force redevelopment kinetics after a rapid length step in intact ferret cardiac muscle, and found that k_{tr} did not vary with activation level in this preparation (Hancock et al., 1993). In the present study we are expanding this investigation by using skinned rat cardiac trabeculae, which allow direct control over myoplasmic

Received for publication 13 December 1995 and in final form 28 February 1996.

Address reprint requests to Dr. Albert M. Gordon, Department of Physiology and Biophysics, School of Medicine, Box 357290, University of Washington, Seattle, WA 98195. Tel.: 206-543-0834; Fax: 206-685-0619; E-mail: amg@u.washington.edu.

0006-3495/96/06/2819/11 $2.00

[Ca^{2+}] and can be compared more closely to the skinned fiber preparation used in skeletal fiber studies. The present work uses feedback control of segment length and two different protocols to drop force: a ramp/restretch (where redevelopment is fit by the rate constant k_{tr}) that compares more closely to previous work in skinned skeletal muscle, and a 4% segment length (L_{seg}) step (where redevelopment is fit by the rate constant k_{step}) similar to the protocol used in our previous work in intact ferret myocardium (Hancock et al., 1993). We find that, consistent with intact cardiac data, k_{tr} and k_{step} do not increase at higher activation levels in skinned cardiac muscle, and stiffness measurements during the redevelopment of force provide strong evidence that the fall and subsequent redevelopment of force are due to cross-bridge detachment and reattachment. When sarcomere length control using laser diffraction is used at submaximum Ca^{2+} levels, a similar lack of activation dependence is found, in contrast with previous reports (Wolff et al., 1995). The present findings are consistent with the steric blocking model of thin filament regulation and are inconsistent with a model of contractile regulation in which Ca^{2+} modulates the kinetics of cross-bridge attachment or detachment.

A preliminary report of this work has appeared in abstract form (Hancock et al., 1994).

MATERIALS AND METHODS

Trabeculae preparation

Male rats (24 rats total, weight 250–350 g) were anesthetized by an intraperitoneal injection of 100 mg/kg body weight pentobarbital sodium (nembutal sodium; Abbott Laboratories, Chicago, IL). Hearts were removed, placed in a dissecting chamber, and bathed in oxygenated physiological salt solution (in mM: 94 NaCl, 24 $NaHCO_3$, 5 KCl, 1 $MgSO_4$, 1 Na_2HPO_4, 0.7 $CaCl_2$). Right ventricles were dissected out in two pieces, pinned down in a petri dish, and stored at −20°C overnight in skinning solution that contained (in mM) 100 KCl, 9 MgCl, 4 MgATP, 5 EGTA, and 10 3-[N-morpholino]propanesulfonic acid (MOPS) with 50% (v/v) glycerol plus 1% Triton X-100. The skinning solution was then replaced by glycerinated relaxing solution (same as skinning without the Triton X-100) and suitable trabeculae were cut free. Each heart yielded approximately 2–4 trabeculae. All procedures involving animals were in accordance with university guidelines.

After the trabeculae were removed from the right ventricle, the ends were trimmed and then chemically fixed using a 2.5% gluteraldehyde solution to reduce the end compliance of the muscle and to improve the grip of the foil end clips (Chase and Kushmerick, 1988). This fixing procedure was identical to that used by Martyn (Martyn and Gordon, 1992), except that bovine serum albumin was not used in the present study. Aluminum foil T-clips (Goldman and Simmons, 1984) were attached to each end of the muscle by folding each arm of the clip over the muscle and crimping it with forceps. Muscles were stored for up to 2 weeks at −20°C. A representative trabecula preparation is shown in Fig. 1.

Solutions

Solutions with varying free Ca^{2+} concentration were mixed using an iterative program that calculates solution composition based on published affinity constants (Martyn and Gordon, 1988). All solutions contained the following (in mM): 95 K^+, 38 Na^+, 1 Mg^+, 3 ATP, 15 CP, 15 EGTA; the dominant anion was propionate and the ionic strength was adjusted to 200 mM with 23–52 mM MOPS buffer. Solutions were adjusted to pH 7.0 at 15°C by titrating with 1 M KOH. For temperature dependence experiments, solutions were adjusted to pH 7.0 at 20° and 30°C. Creatine phosphokinase (CPK) (0.25 mg/ml; Sigma Chemical Company, St. Louis, MO) was added to each solution on the day of the experiment. All solutions were used at 15°C, except where noted.

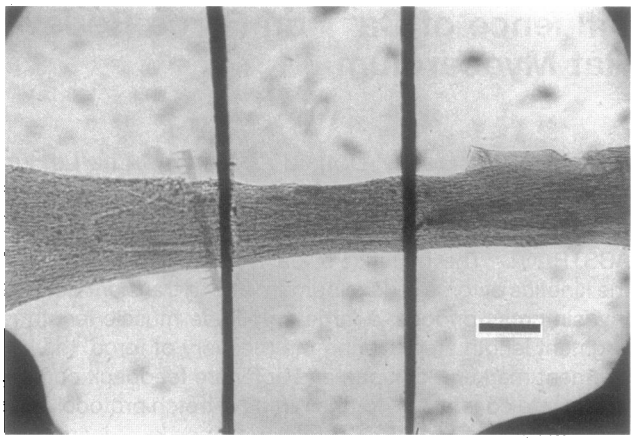

FIGURE 1 Skinned rat trabecula preparation under relaxing conditions (pCa 9.2) showing segment markers. Calibration bar is 200 μm.

Mechanics apparatus

The muscle mechanics setup consisted of a shaker motor (Ling model 300), a force transducer (Akers model AE801; Senso-nor), and accompanying electronics hardware. A PC 486/33 clone running customized software was used to control the motor position during an experiment and to acquire the data. For solution changes, a simple system using a 1-ml syringe and a small valve was employed such that new solution was injected into one end of the chamber and the old solution was removed by suction at the other end. The chamber volume was 100 μl.

Segment and sarcomere length measurement

Although laser diffraction has been used to measure sarcomere length in skinned cardiac muscle, at the highest levels of activation the first-order diffraction maxima decrease in intensity and display increased dispersion (Kentish et al., 1986), making it difficult to effectively use feedback control. Because accurate determination of isometric force redevelopment kinetics requires control of sarcomere length (Brenner and Eisenberg, 1986), we designed a segment measurement technique using a pair of aluminum foil markers to delineate a central segment of the muscle (30–40% of muscle length). The presumption is that changes in segment length accurately correlate with changes in sarcomere length within the segment. Foil markers approximately 25 μm wide and 1.5 mm long were folded in half, placed around the muscle, and gently crimped with forceps to attach them to the muscle perpendicular to the muscle axis, as shown in Fig. 1. These segment markers were then imaged with white light, and the image was split with a 90° mirror onto a pair of 256-element photodiode arrays (PDA) (Reticon, Sunnyvale, CA) with each PDA imaging one marker. To optimize the optical signal from each marker and to minimize the effect of marker skewing (which was occasionally seen at high activation levels), half-cylinder lenses were used to compress the length of the marker on each PDA. To maximize resolution, the centroid of each marker was determined electronically to give the marker position along the PDA. The absolute length of the segment was determined visually, and changes in segment length were calculated from changes in the photodiode array output signals. The resolution of the segment length detection system was approximately 0.5 μm.

In ventricular cardiac muscle passive tension rises steeply above sarcomere lengths of roughly 2.25 μm, such that sarcomere length cannot be extended beyond approximately 2.35 μm without irreversibly damaging the muscle (Huntsman et al., 1983; Kentish et al., 1986). Similarly, we found that segment marker spacing could not be extended beyond a certain length without very high levels of passive tension. Thus, the maximum segment length ($L_{seg(max)}$) was defined as the segment length beyond which further increases in muscle length cause no change in segment length; segment length was expressed as a percentage of $L_{seg(max)}$.

To verify the correlation between sarcomere length within the segment and segment marker spacing, segment length and sarcomere length were measured in parallel in five muscles at a series of muscle lengths and submaximum Ca^{2+} levels. Sarcomere length was determined by illuminating the region of the muscle between the segment markers with a 3-mW He-Ne laser (Melles-Griot, Boulder, CO) and measuring the position of both first-order diffraction maxima using the same optical detection system as for segment length measurements (for further details see Martyn and Gordon, 1992). The relationship between sarcomere length and segment length for one muscle at various levels of calcium activation is shown in Fig. 2. A linear relationship between segment length and sarcomere length was found for data from each of five muscles; when data for each muscle at all pCa's were individually fit by linear regression, the average slope was 44.6 ± 6.27% L_{seg}/μm, the average intercept was −6.59 ± 16.4% L_{seg} (both mean ± SD), and the correlation coefficients ranged from 0.957 to 0.992.

Because of the high quality and reliability of the segment marker signal, it was possible to use real-time feedback control of segment length, such that the muscle length was altered to keep the segment length constant during force redevelopment experiments. Segment length was sampled at 2 or 4 kHz and compared to a reference level in software; the muscle length was varied to minimize the difference between the segment length signal and the segment length reference. The software feedback system provided sufficient bandwidth to maintain segment length isometric conditions during the period of force redevelopment. This feedback system was also used to control sarcomere length (obtained by He-Ne laser diffraction) at submaximum force levels.

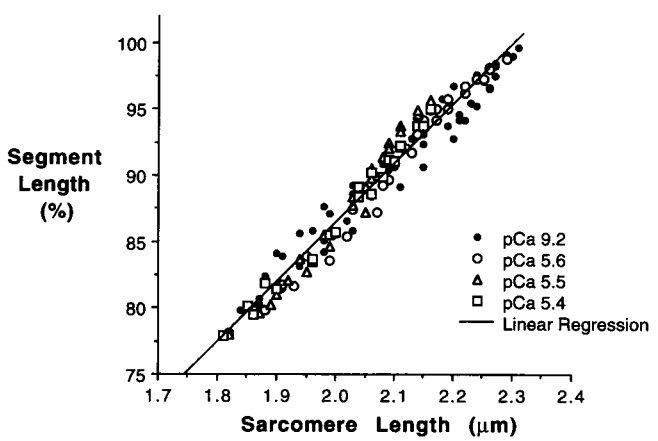

FIGURE 2 Sarcomere length versus segment length for one muscle. Calcium-activated forces (relative to maximum force) were as follows: 6% at pCa 5.6, 22% at pCa 5.5, 32% at pCa 5.4. Maximum sarcomere length for this muscle was 2.32 μm. The least-squares linear regression to data at all pCa's (*solid line*) has a slope of 44.8% L_{seg}/μm, a y-intercept of −3.36% L_{seg}, and r = 0.980. Similar data were found for four other muscles. Protocol: The muscle is stretched to $L_{seg(max)}$ and then activated, which causes segment length to shorten to 90–95%. Segment length is then measured at set increments of ML as the muscle is shortened to its minimum length and stretched to its maximum extension. After the optics are rearranged, sarcomere length measurements are made at the same ML increments and compared to the segment length data. The procedure is repeated at different pCa levels.

Mechanical perturbations

For the force redevelopment measurements, two protocols were used to rapidly drop force and detach cross-bridges. The first technique (the ramp/restretch protocol) consists of a large amplitude ramp (15 to 20% muscle length (ML) at a ramp rate of 4 to 6 ML/s) followed by a rapid (approximately 1.5 ms) restretch of the muscle back to the original segment length. The second technique (the step protocol) employs a 4% segment length step (which takes 5 ms to complete) to drop the force. For the ramp/restretch technique, the segment length clamp is engaged within 1 ms after the restretch such that the segment length is held constant for the duration of force redevelopment. For the step technique, the segment length clamp is engaged 50 ms before the step and is in effect for the entire force redevelopment period; the segment length step is achieved by changing the segment length command level at a specified time. All data were taken between 90% and 100% $L_{seg(max)}$.

For comparison, ramp/restretch data using sarcomere length control were taken from a subset of muscles; in this case the sarcomere length clamp was engaged immediately after the restretch to maintain a constant sarcomere length for the duration of force redevelopment.

Data analysis

The redevelopment of force after the ramp/restretch or 4% segment length step was fit by a mono-exponential function of the form

$$\text{Force} = a * (1 - e^{-k_{tr}*t}) + b,$$

where a is the redeveloped force, b is the offset from which force redevelops, k_{tr} (or k_{step}) is the exponential rate constant, and t is time. The data were fit using customized software that employed the Simplex algorithm (Caceci and Cacheris, 1984) to optimize the least-squares fit. Because of noise on the force traces, approximately the first 50 ms of the force redevelopment after the restretch and the first 5 ms after the segment length step were excluded from the fits, and fits where the value of a was less than 3 mg were excluded because the noise on the force trace at these low force levels prevented unequivocal interpretation of the exponential fits. Data were generally well fit by a mono-exponential.

Maximum force, taken at pCa 4.6 or 5.0, was measured periodically during the experiment to determine the decline of maximum force, and steady-state force at various pCa levels was normalized to maximum force at pCa 4.6 or 5.0. Because longer activation times resulted in greater deterioration in force, efforts were made to minimize the length of Ca^{2+} activations; experiments were terminated when maximum force fell to less than 60% of the initial level.

Stiffness measurements

Sinusoidal stiffness during force redevelopment was measured by imposing a 400-Hz sinusoidal change in muscle length and monitoring the resulting sinusoidal fluctuation in force and segment length using a pair of lock-in amplifiers (model 3961B; Ithaco, Ithaca, NY). The amplitude of the sinusoids was constant for a given trial and varied from 0.20 to 0.70% ML. With this arrangement, one amplifier detected the amplitude of the force fluctuations and the other amplifier detected the amplitude of the segment length fluctuations; stiffness was defined as the instantaneous ratio dF/dL_{seg}. To improve signal quality, internal band-pass filters with center frequency of 400 Hz and Q = 1 were used for both signals. For a subset of the data, the peak-to-peak force and L_{seg} fluctuations were determined manually and compared to the lock-in amplifier signals; this analysis gave similar results.

RESULTS

Force redevelopment data using segment length control were taken from a total of 22 muscles (with step data taken

from 21 of 22 and ramp/restretch data taken from 22 of 22). The muscle dimensions were (mean ± SD): muscle length, 2.05 ± 0.49 mm; width, 203 ± 62 μm; segment length, 684 ± 128 μm. Muscle thickness was estimated by rotating the muscle along its axis under the dissecting microscope and finding the minimum dimension; thickness was found to be on average one-third of the muscle width, as observed by others (Kentish et al., 1986). Assuming an elliptical cross section, maximum Ca^{2+}-activated force was 74.2 ± 24.2 mN/mm^2 (mean ± SD) at 95% L_{seg}. Force redevelopment after a ramp/restretch was measured using sarcomere length control at submaximum Ca^{2+} levels in a separate series of seven muscles. The mean (± SD) muscle lengths, widths, and maximum Ca^{2+}-activated force for these muscles were 1.54 ± 0.36 mm, 171.6 ± 38.1 μm, and 73.0 ± 35.1 mN/mm^2, respectively.

Ramp/restretch data

Representative traces of force, segment length, and muscle length after a ramp/restretch with segment length control are shown in Fig. 3 *A*; corresponding traces using sarcomere length control at submaximum Ca^{2+} are shown in Fig. 3 *B*. To determine whether there was any activation dependence of k_{tr}, data pooled from all muscles using segment length control were plotted both as a function of pCa (Fig. 4 *A*) and as a function of relative force (Fig. 4 *B*). For comparison, k_{tr} measurements obtained with sarcomere length control are included in Fig. 4 *B*. For k_{tr} obtained using either segment or sarcomere length control, the slope of a regression line fit to either the raw or the binned data was not significantly different from zero ($p < 0.05$, Student's *t*-test), demonstrating that k_{tr} after the ramp/restretch is independent of the level of Ca^{2+} activation. Furthermore, at a given force level there was no significant difference ($p < 0.05$, Student's *t*-test) between k_{tr} obtained with sarcomere control or segment control. Because deterioration of the sarcomere length signal at maximum activation precluded sarcomere length clamp measurements of k_{tr}, all other data were obtained with the segment technique.

The ramp/restretch protocol did not cause force to drop to the baseline; instead, force fell to approximately 60% of the initial force and redeveloped to steady state from there. In skeletal muscle a similar protocol has been found to drop force to zero (Brenner, 1988), although in some cases a force offset after restretch is observed in skeletal muscle (Burton, 1991). In the present study, the force offset varied both for different tests in a given muscle and between muscles, although k_{tr} did not vary consistently with changes in the force offset, even when the offset was as low as 20%. When the force offset was expressed relative to total force, there was no consistent variation with either the pCa or the segment length at which the redevelopment was measured.

In parallel with the segment length clamped ramp/restretch data, unclamped (ML control) ramp/restretch data were acquired at all activation levels for a subset of the muscles. Although preliminary experiments suggested a moderate activation dependence of unclamped ramp/restretch k_{tr}, the measurements performed in conjunction with the present segment length clamped data did not show

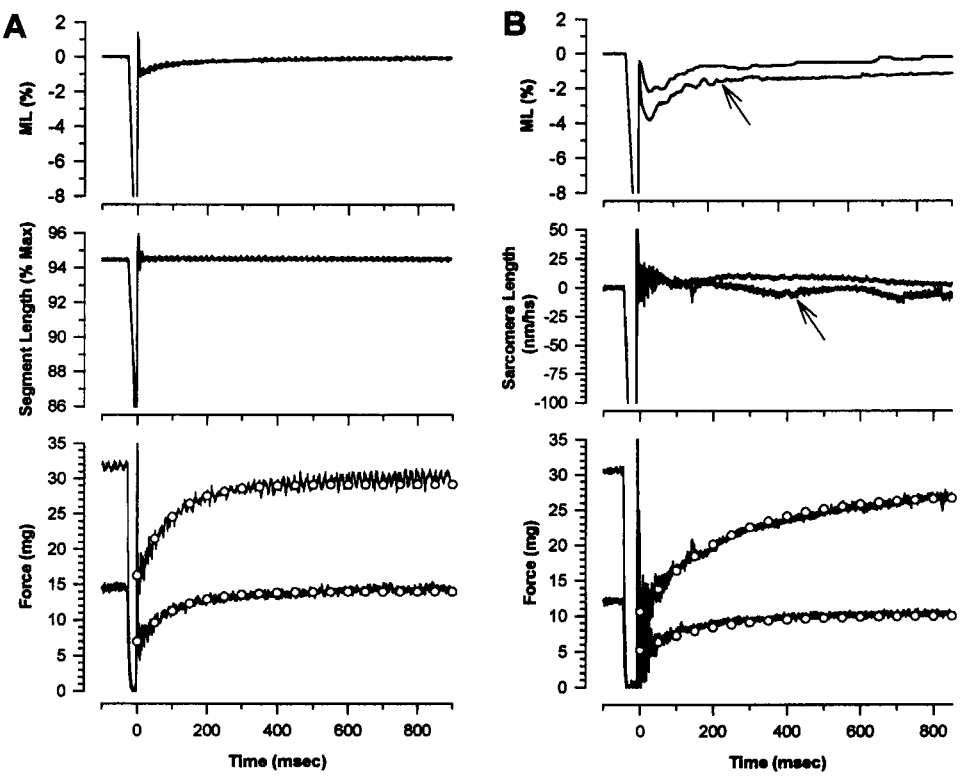

FIGURE 3 Representative traces of muscle length (*top panels*), segment or sarcomere length (*middle panels*), and force (*bottom panels*) obtained during the ramp/restretch protocol during (*A*) segment length and (*B*) sarcomere length control measurements of k_{tr}. In *B* the initial sarcomere length was 2.18 μm, corresponding to 93% of the maximum sarcomere length in this muscle. To facilitate comparison of segment and sarcomere length traces, the sarcomere length axis in the middle panel in *B* corresponds to a range of 10% sarcomere length. Data were obtained at pCa 5.3 (30% maximum force) and 5.2 (64% maximum force) in *A* and at pCa 5.8 (32% maximum force) and 5.7 (58% maximum force) in *B*. The exponential fits to each force trace are indicated by open circles. In *B* the muscle length and sarcomere length traces corresponding to data obtained at pCa 5.7 are indicated by arrows.

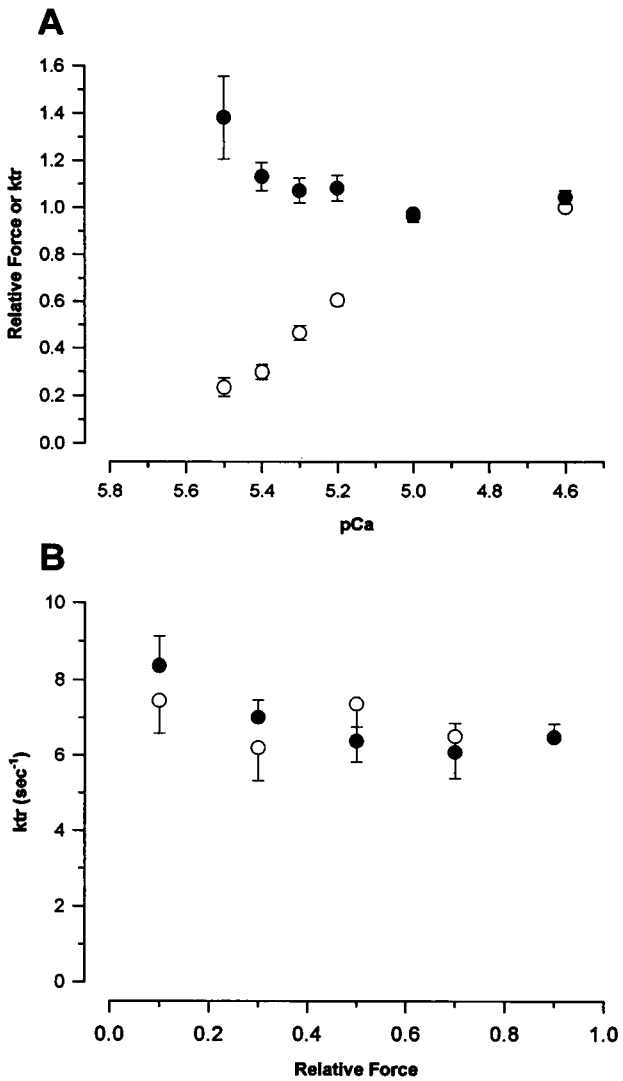

FIGURE 4 Pooled force redevelopment data for ramp/restretch protocol with segment length and sarcomere length control. In *A* normalized force (○) and normalized k_{tr} (●), obtained with the segment length control protocol, are plotted as a function of pCa. k_{tr} was normalized to average k_{tr} at relative force = 1.0 for each muscle; force was normalized to maximum Ca^{2+}-activated (mean ± SEM; N = 17 muscles). In *B* average k_{tr} is plotted as a function of normalized force obtained at different pCa's. Data for segment length (●) and sarcomere length (○) controlled protocols are shown. Data were segregated into five bins based on their relative force level, and the average value for k_{tr} is plotted (mean ± SEM, N = 22 muscles for segment length control; N = 7 muscles for sarcomere length control). The number of measurements in each bin from lowest to highest relative forces are 39, 38, 55, 31, and 115 for segment control data (●) and 14, 41, 16, and 16 for sarcomere control data (○). k_{tr} data are weighted to the number of total determinations for each muscle.

any activation dependence. In fact, the unclamped ramp/restretch results were similar to the clamped ramp/restretch results shown here, with the exception that there was more scatter in the k_{tr} values and the relative redeveloped force was smaller for the unclamped data. Because of the large degree of segment length shortening during redevelopment, unclamped segment length steps were not studied.

Step data

Representative traces of muscle length, segment length, and force during the step protocol are shown in Fig. 5 *A*. The steep dependence of force on sarcomere length in cardiac muscle is reflected by the difference between the initial and the final steady-state force levels. Pooled k_{step} data from a total of 21 muscles are shown both as a function of pCa (Fig. 5 *B*) and as a function of relative force (Fig. 5 *C*). When a regression line was fit to the raw data, the slope was small ($-3.35\ s^{-1}/F_{rel}$, corresponding to a 21% fall in k_{step} over the entire range of relative force), but was significantly different from zero ($p > 0.05$, Student's t-test). Importantly, there is no positive activation dependence of k_{step}.

Effect of muscle size on force redevelopment measurements

We investigated the possibility that an activation dependence of k_{tr} might be masked because of variations in muscle size. For example, if the diffusion of ATP into the center of the larger preparations was too slow to keep up with ATP consumption, or if there was a buildup of inorganic phosphate (P_i) in the center of the muscles, this could change the contraction kinetics of these larger muscles. To test this possibility, the activation dependence of k_{tr} (where dk_{tr} = [average k_{tr} at F_{max}]/[average k_{tr} for all forces less than 50% F_{max}]) for each muscle was plotted as a function of muscle width (Fig. 6). Note that because the thickness of these preparations was approximately one-third of the width, the diffusion distances are considerably smaller than the muscle widths may suggest. As can be seen, the three muscles that showed a positive activation dependence for k_{tr} were below 200 μm width; however, there were 10 other muscles with width 200 μm or less that displayed either no activation dependence or a negative activation dependence for k_{tr}. For the step protocol, no muscles showed a positive activation dependence of $dk_{step} > 1.1$.

Comparison of the magnitudes of k_{tr} and k_{step}

When k_{tr} and k_{step} values were averaged over all pCa for each muscle, there was substantial muscle-to-muscle variation: k_{tr} varied from 2.6 to 12.6 s^{-1} and k_{step} varied from 7.5 to 24.5 s^{-1}. The basis of this variability is not clear, and muscles from a single heart displayed similar variability, indicating that animal-to-animal differences were not responsible. Furthermore, the variability did not correlate with muscle size or geometry. One factor that may contribute to the range of observed values is differences in relative myosin isoform composition between muscles, although based on dynamic stiffness (Rossmanith et al., 1986) and myosin ATPase measurements (VanBuren et al., 1995), isoform differences would not be expected to account for more than a twofold variation. A second variable is differences in the extent of protein phosphorylation between various muscles, as phosphorylation of myosin light chain 2 has been shown

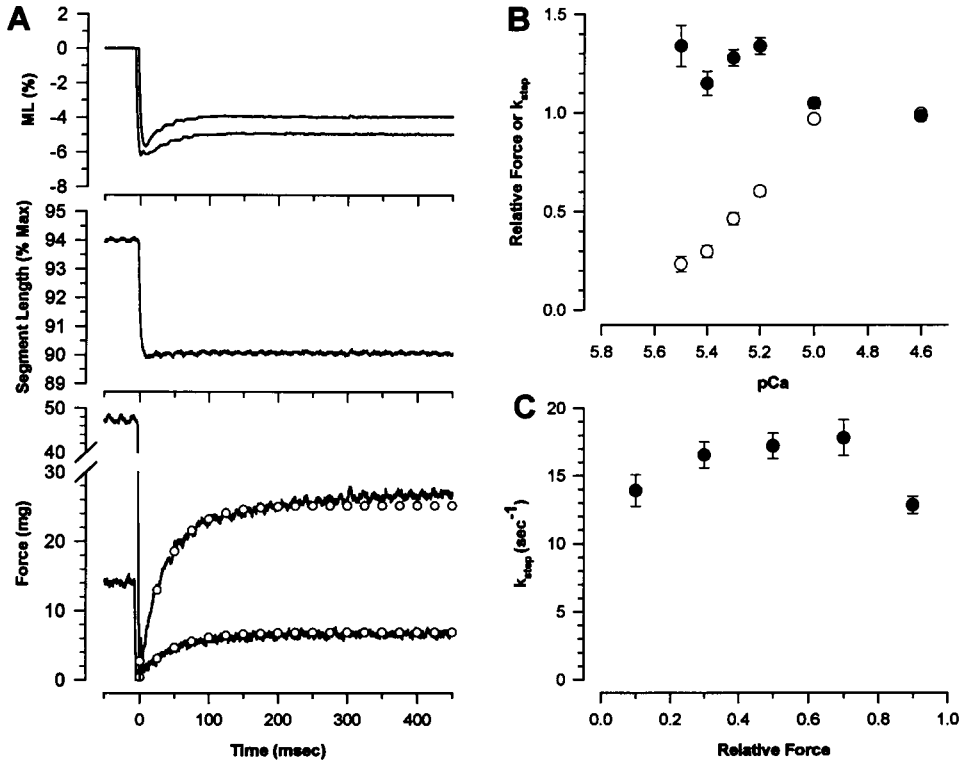

FIGURE 5 (*A*) Representative traces of muscle length (*top*), segment length (*middle*), and force (*bottom*) obtained during the step protocol at pCa 5.3 (30% maximum force) and 5.0 (100% maximum force). Single exponential fits to the force traces are indicated by open circles. (*B*) k_{step} was normalized to the value of k_{step} at relative force = 1.0; force was normalized to the maximum Ca^{+2}-activated value (mean ± SEM; N = 17 muscles). (*C*) Average k_{step} is plotted as a function of normalized force obtained at different pCa's (mean ± SEM; N = 21 muscles). Data were segregated into five bins based on their relative force level, and the average value for k_{step} is plotted. The number of measurements in each bin from lowest to highest relative forces is 27, 35, 47, 30, and 106. k_{step} data are weighted to the number of total determinations for each muscle.

to elevate k_{tr} at submaximum activation levels in skeletal fibers (Metzger et al., 1989; Sweeney and Stull, 1990). These issues were not explored in the present study.

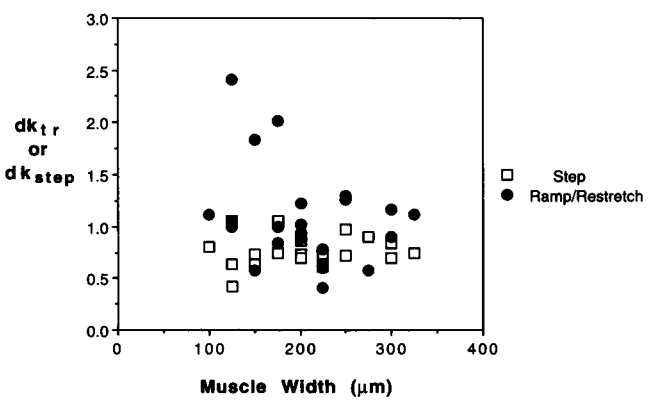

FIGURE 6 Activation dependence of k_{tr} and k_{step} as a function of muscle width. For each of 22 muscles, average k_{tr} at relative force = 1.0 and average k_{tr} at relative force < 0.5 were compared, and dk_{tr} was calculated for each muscle as (average k_{tr} @ relative force = 1.0)/(average k_{tr} @ relative force < 0.5). Similar calculations were made for k_{step}. Between 1 and 12 points were used for each average k_{tr} or average k_{step}, and standard deviations of dk_{tr} and dk_{step} (not shown) averaged 0.44 and 0.39, respectively.

Although neither k_{tr} nor k_{step} varied positively with activation level, the ramp/restretch and the step protocols gave different quantitative results: when averaged for all muscles at all pCa levels, average k_{tr} was 7.06 ± 3.16 s^{-1} (mean ± SD for 278 determinations from 22 muscles) and k_{step} was 15.7 ± 5.67 s^{-1} (mean ± SD for 245 determinations from 21 muscles). A number of possible reasons for this difference in the magnitudes of k_{tr} and k_{step} were tested.

The first possibility is that the difference in segment length at which force redevelops in the two protocols is the cause of the discrepancy between k_{tr} and k_{step}: for the ramp/restretch, force redevelops at the initial L_{seg}, whereas for the step protocol force redevelops at 4% below the initial L_{seg}. To test this idea, a normal ramp/restretch protocol was modified so that instead of stretching back to the original L_{seg}, the restretch returned to 4% below the initial L_{seg} and force was allowed to redevelop at the shorter length. This protocol gave k_{tr} values that were not statistically different ($p < 0.05$, Student's unpaired t-test) from the normal ramp/restretch values (k_{tr} = 5.24 ± 1.69 (mean ± SD), N = 17 determinations from two muscles for standard ramp/restretch; k_{tr} = 6.10 ± 1.65 (mean ± SD), N = 14 determinations from the same two muscles for ramp/restretch with 4% offset), indicating that the difference between the

magnitudes of k_{tr} and k_{step} was not due to the difference in segment length.

The second difference between the two protocols is the duration of the unloaded shortening preceding force redevelopment. The segment length step is quite rapid (5 ms or less) and the duration of unloaded shortening is very short. On the other hand, the ramp/restretch protocol provides a 30- to 40-ms duration of unloaded shortening before the muscle is stretched back to its original length. To test the importance of unloaded shortening duration, a release/restretch protocol was devised in which a large-amplitude (15 or 20%) ML step was used instead of the ramp, and the duration of this release was varied from 10 to 100 ms; k_{tr} was measured after the restretch back to the original L_{seg}. Release/restretch perturbations of 25 or 50 ms gave k_{tr} values similar to the 25 or 50 ms ramp/restretch protocols, indicating that for the purposes of force redevelopment, the ramp and the release were equivalent. However, when the duration of the release was shortened to 10 ms, a faster value of k_{tr} was obtained (Fig. 7), demonstrating that the duration of unloaded shortening influences the rate of the subsequent force redevelopment. Therefore, differences in the duration of unloaded shortening preceding force redevelopment may explain the disparity between the magnitudes of k_{tr} and k_{step}.

Stiffness changes during force redevelopment

To further investigate the nature of the processes occurring during force redevelopment, sinusoidal stiffness was measured during the rise of force after step and ramp/restretch protocols. The stiffness measurement served two purposes. First, because stiffness is thought to be a measure of cross-bridge attachment, this analysis constituted a test of whether the mechanical perturbations designed to drop force also led to cross-bridge detachment and whether force redevelopment coincided with cross-bridge attachment. Second, the stiffness measurement provided a way to check whether the difference in the magnitudes of k_{tr} and k_{step} resulted from differences in the degree of cross-bridge detachment. When relative stiffness is plotted as a function of relative force during redevelopment (Fig. 8), the data for the two protocols lie near the unity line, suggesting that force and cross-bridge attachment are proportional during the redevelopment of force. For the ramp/restretch protocol (Fig. 8 *A*), stiffness at 50% maximum force corresponds to the force

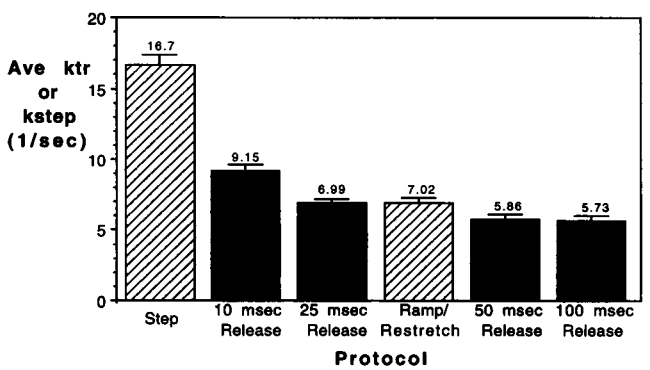

FIGURE 7 k_{tr} or k_{step} averaged over all pCa levels as a function of protocol used to drop force. In addition to the ramp/restretch and step protocols (*cross-hatched bars*), data are shown for a release/restretch protocol with varying release durations from 10 to 100 ms (*solid black bars*). The release/restretch protocol is identical to the ramp/restretch protocol, except that instead of a 15–20% ML ramp with duration 33 or 37 ms, it consists of a 15–20% ML release with a variable time interval at the short length. Data are given as mean ± SEM for six muscles. Note that duration of the step is approximately 5 ms and duration of the ramp/restretch is 33 or 37 ms (depending on muscle).

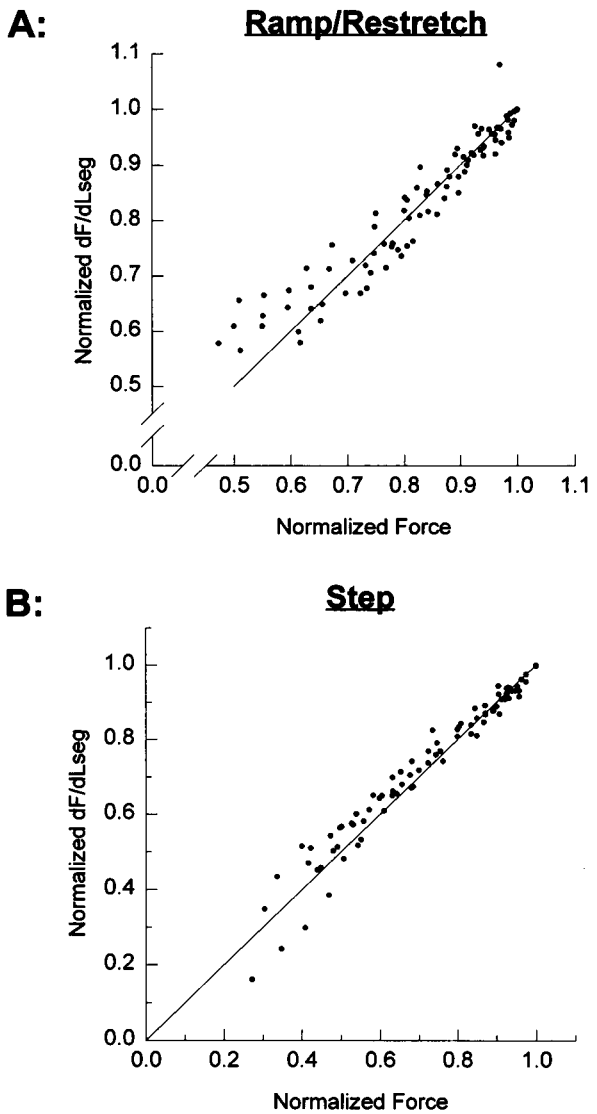

FIGURE 8 Relative sinusoidal stiffness versus relative force during force redevelopment after ramp/restretch (*A*) and step (*B*) protocols. Stiffness was measured at pCa 4.6 using a 400-Hz sinusoid as described in text; data are from eight traces (*A*) and seven traces (*B*) from four muscles. Force, dF, and dL_{seg} data during redevelopment were averaged over 10-ms (earlier times) or 20-ms (later times) time windows. Stiffness was taken as dF/dL_{seg} at each time, and force and stiffness were normalized to values at the plateau of redevelopment.

offset after restretch and suggests that the force offset is due to cross-bridge attachment. For the step protocol (Fig. 8 *B*), the lowest force level at which stiffness could be measured was approximately 25%, indicating that force and stiffness are proportional, at least down to 25% relative force.

Influence of temperature

Finally, the temperature dependence of force redevelopment kinetics was examined by measuring k_{tr} at 20°C and 30°C at pCa 4.6 in three muscles. At 30°C the ramp/restretch k_{tr} was 30.3 ± 6.42 s^{-1} (mean ± SD of 11 determinations from three muscles), and k_{step} was 53.6 ± 19.4 s^{-1} (mean ± SD of 13 determinations from three muscles). The Q_{10} values, defined as (average k_{tr} at 30°C)/(average k_{tr} at 20°C) for each muscle, were 3.3 ± 0.53 (mean ± SD from three muscles) and 3.2 ± 0.61 (mean ± SD from three muscles) for k_{tr} and k_{step}, respectively, suggesting that the two rates are characteristic of the same enzymatic process.

DISCUSSION

The present results establish that the kinetics of force redevelopment do not increase with the level of Ca^{2+} activation in skinned cardiac muscle. This lack of activation dependence of k_{tr} has now been observed in intact cardiac muscle (Hancock et al., 1993) and in skinned myocardium using two mechanical perturbations to detach cross-bridges, and using both segment length and sarcomere length control. The data are consistent with a Ca^{2+} activation model in which Ca^{2+} modulates the number of thin filament units that can interact with myosin cross-bridges, and are inconsistent with a model in which Ca^{2+} modulates the rate of myosin cross-bridge attachment.

Ramp/restretch protocol

The purpose of the ramp/restretch and the step perturbations was to shift the population of cycling cross-bridges toward detached or weakly bound states, so that cross-bridge reattachment or transitions to strongly bound states could be monitored by measuring the redevelopment of force. The ramp/restretch protocol was developed to reduce the number of attached cross-bridges during shortening, followed by a restretch back to the original length to forcibly detach any remaining cross-bridges (Brenner, 1988; Metzger and Moss, 1990). In skeletal muscle this mechanical protocol generally drops force to near zero, although in some cases there is a small force offset immediately after the restretch (Burton, 1991; Metzger et al., 1989). In the ramp/restretch protocols used here for cardiac muscle, however, there was a consistent force offset after the restretch, such that the redeveloped force was always less than the total force (Fig. 3).

A possible explanation for the nonzero force offset is that passive tension is responsible; in cardiac muscle passive tension rises steeply above sarcomere lengths of 2.25 μm (approximately 93% segment length) (Huntsman et al., 1983; Kentish et al., 1986). However, this notion is contradicted by the finding that when the ramp/restretch was performed at shorter segment lengths (below 90%), where passive tension is negligible, the force from which the redevelopment takes off was no smaller. Second, if passive tension were responsible for the nonzero offset, then the relative offset as a fraction of the total force would be larger at lower activation levels. This is not the case; instead, the relative redevelopment fraction was independent of the total force level.

When sinusoidal stiffness was measured during force redevelopment, stiffness was found to be proportional to force for the entire redevelopment duration (Fig. 8). This finding indicates that force is a good index of cross-bridge attachment during redevelopment, and suggests that the force offset after the restretch is in fact due to residual cross-bridge attachment.

Does residual cross-bridge attachment affect k_{tr} measurements?

The force offset in the ramp/restretch protocol raises the possibility that cross-bridge attachment after the restretch leads to residual thin filament activation, which masks the activation dependence of k_{tr}. For example, it has been suggested (Wolff et al., 1995) that if residual attached cross-bridges activated the thin filament, the degree of activation that could be modulated by changing myoplasmic $[Ca^{2+}]$ would be diminished, resulting in the apparent lack of Ca^{2+} sensitivity of k_{tr} observed in intact myocardium (Hancock et al., 1993). This explanation is unlikely, however, because the steady-state force varies with pCa and the force offset after restretch is a constant proportion of steady-state force (see Fig. 3), so the level of residual thin filament activation after the restretch will also vary with pCa. Thus, at the lowest activation levels the amount of residual cross-bridge attachment, as measured by the force offset after the restretch, is less than 15% of maximally activated force. An activation dependence, if present, should therefore be detectable because k_{tr} is measured at a range of activation levels; this is especially true, because in fast and slow skeletal muscle virtually all of the variation in k_{tr} occurs at the highest 30–40% force levels (Brenner, 1988; Chase et al., 1994; Metzger and Moss, 1990; Millar and Homsher, 1990).

The second issue is whether the residual thin filament activation is sufficient to "turn on" k_{tr} to its highest level, even at low $[Ca^{2+}]$. This idea is discounted by two pieces of evidence. First, our observation that k_{step} does not increase with activation level (Fig. 5 *B*), although force redevelops from near zero after the step, indicates that force offsets do not influence force redevelopment measurements significantly. Second, recent measurements of force redevelopment in skinned myocardium after photolytic release of caged Ca^{2+} (where the rise of force is described by the rate

constant k_{Ca}, analogous to k_{tr}) found that k_{Ca} was activation dependent, despite significant levels of steady-state force preceding Ca^{2+} release (Araujo and Walker, 1994). These results suggest that a moderate degree of steady submaximum force preceding redevelopment does not completely "turn on" k_{Ca} or k_{tr}.

Potential effects of nucleotide and P_i gradients on k_{tr} measurements

Because cardiac trabeculae are multicellular preparations which, in general, are larger in diameter and thickness than skinned skeletal muscle fibers, it is possible that long diffusion paths from the bathing media to the center of the preparations could result in radial gradients of nucleotides and phosphate during active force generation. For example, the effect of elevated myoplasmic $[P_i]$ on force in skinned rat trabeculae has been found to vary with preparation dimension (Kentish, 1986). Because elevated $[P_i]$ increases k_{tr} in skinned skeletal fibers (Metzger and Moss, 1991), progressive increases of myoplasmic $[P_i]$ with increasing activation levels could affect our measurements of k_{tr}. However, the magnitudes of k_{tr} and k_{step} at maximum calcium activation do not vary with muscle width (data not shown), suggesting that either the elevation of $[P_i]$ was insufficient to significantly affect k_{tr} or that elevated $[P_i]$ does not alter isometric force redevelopment kinetics in cardiac muscle.

Although ATP gradients can result from active cross-bridge cycling in larger skinned muscle preparations (Chase and Kushmerick, 1995), it is unlikely that significant metabolite gradients affect our results for the following reasons. First, our solutions contained an ATP regenerating system consisting of 3 mM ATP buffered by 15 mM CP and 0.25 mg/ml CPK. Second, metabolite gradients are smaller than might be expected from the width measurements because the muscle thickness was approximately one-third of the width. A third factor that should reduce the gradients is the slow ATPase rate expected at the experimental temperature of 15°C, relative to comparable studies performed at 24°C (Kentish and Stienen, 1994). Finally, compared to skinned skeletal preparations, the myofibrillar protein content of an equal volume of ventricular cardiac muscle is significantly less (Eisenberg, 1983). Thus, it is improbable that ATP gradients are large enough to influence our results, a conclusion that is supported by the data shown in Fig. 6. If a strong positive activation dependence of k_{tr} were masked by ATP depletion in the core of larger trabeculae at high levels of activation, the activation dependence of k_{tr} would decrease as width increases. The data in Fig. 6 clearly indicate that this is not the case.

Disparity in the magnitudes of k_{tr} and k_{step}

Although both the ramp/restretch and the step protocols appear to detach cycling cross-bridges, it is unclear why the magnitudes of k_{tr} and k_{step} are different (i.e., 16 s^{-1} vs. 7 s^{-1}). The first obvious difference is that force redevelops from a nonzero offset for the ramp/restretch protocol, whereas force redevelops from near zero for the step protocol. From this offset, one could propose that the remaining attached cross-bridges somehow lead to a slower force redevelopment rate for the ramp/restretch protocol. However, when the step amplitude was reduced from 4% to 2% or 1% L_{seg}, leading to a residual force offset, presumably due to incomplete cross-bridge detachment, k_{step} was faster than for the 4% step (data not shown). These faster rates in fact are expected if force redevelopment in this case is dominated by force-generating transitions of attached cross-bridges (Huxley and Simmons, 1973), and suggests that residual cross-bridge attachment leads to faster rather than slower redevelopment kinetics.

When the duration of unloaded shortening preceding force redevelopment was reduced, k_{tr} increased (Fig. 7). One possible explanation for the dependence of k_{tr} on the duration of unloaded shortening preceding it is that Ca^{2+} bound to TnC dissociates during the unloaded phase, and more Ca^{2+} dissociates for longer release durations. In cardiac muscle rapid length releases lead to a rise in myoplasmic $[Ca^{2+}]$ in both intact (Backx and ter Keurs, 1993) and skinned (Allen and Kentish, 1988) myocardium, which presumably results from a decreased affinity of TnC for Ca^{2+}. If longer periods of unloaded shortening allowed more Ca^{2+} to be released from TnC, subsequent force redevelopment could be slowed. However, this explanation is unlikely because when the amount of Ca^{2+} bound to TnC is reduced by lowering the free $[Ca^{2+}]$ in solution, k_{tr} does not decrease (Figs. 4 and 5).

Relation to previous studies

By measuring isometric force development in cardiac muscle after flash photolysis of caged Ca^{2+}, others have observed a three- to fourfold activation dependence of myocardial force development kinetics (Araujo et al., 1993; Barsotti et al., 1994). However, it must be remembered that the rise in force after rapid Ca^{2+} release involves at least two coupled kinetic processes, i) Ca^{2+} binding and thin filament activation and ii) cross-bridge attachment and transition to force-generating states. On the other hand, we measured force redevelopment under steady-state activation. Thus, the result that k_{tr} is independent of activation on the one hand, whereas k_{Ca} exhibits an activation dependence, may not be contradictory. To sort out these differences, it will be necessary to determine the rate of Ca^{2+} binding to the cardiac thin filament or the rate of thin filament activation after a step increase in myoplasmic $[Ca^{2+}]$.

The activation dependence of cross-bridge cycling rates in cardiac muscle has also been inferred from dynamic stiffness analysis (Shibata et al., 1987) and pseudo-random binary noise modulated length perturbations (Hoh et al., 1988; Rossmanith et al., 1986). In these studies the fre-

quency of minimum stiffness, f_{min}, is used as an index of cross-bridge kinetics. Whereas f_{min} is found to vary with temperature (Rossmanith et al., 1986), β-adrenergic stimulation (Hoh et al., 1988), and myosin isoform type (Rossmanith et al., 1986), f_{min} is independent of the level of activation (Shibata et al., 1987). These data are consistent with our finding that force redevelopment kinetics do not vary with activation level in mammalian cardiac muscle.

Recent measurements of k_{tr} in skinned rat trabecular muscle indicate that k_{tr} varies nearly fourfold with the level of Ca^{2+} activation (Wolff et al., 1995), in sharp contrast to the results in this study. The values of k_{tr} obtained at maximum Ca^{2+}-activated force are similar to ours (9.51 s^{-1} versus 6.48 s^{-1}). However, there are several differences between the two studies. We utilized a segment marker technique for length control, whereas Wolff et al. used an iterative sarcomere length control technique in which the desired sarcomere length was approximated in a series of transients. As discussed above, we were able to implement real-time control of sarcomere length at force levels up to 65% of maximum and found that the results over that range of forces were very similar to those obtained with segment length control (Figs. 3 and 4 *B*). The results of Wolff et al. indicate that over the range of force from 20 to 65% of maximum, k_{tr} would increase by a factor of 2, yet we did not find such an increase when using either segment length or sarcomere length control (Fig. 4 *B*). A second difference between these studies was the use of CPK (0.25 mg/ml) in all fiber solutions in this study, whereas CPK was not added to solutions in the study by Wolff et al. This is potentially an important difference because during tension redevelopment, the transitions of cross-bridges from detached or weak binding states to strongly bound, force-producing cross-bridge states have been shown to be sensitive to changes in nucleotide or P_i levels.

The present results are consistent with our previous measurements of force redevelopment kinetics in tetanized intact ferret right ventricular papillary muscle (Hancock et al., 1993). In that study, k_{tr} did not vary with activation, and the magnitudes of k_{tr} were on the order of 60 s^{-1} at 27°C. The step protocol used in the present study is very similar to the protocol used in the intact study, and k_{step} values are on the order of 16 s^{-1} at 15°C and 54 s^{-1} at 30°C. Although direct quantitative comparisons are complicated by myosin isoform differences between rat hearts and ferret hearts, the important similarity is that k_{step} does not increase with activation level in both skinned rat and intact ferret myocardium.

The kinetics of force redevelopment after release and restretch has been found to vary nearly tenfold from submaximum to maximum Ca^{2+} activation levels in fast skeletal fibers (Brenner, 1988; Metzger and Moss, 1990) and approximately fourfold in slow skeletal fibers (Metzger and Moss, 1990). In the present study k_{tr} does not vary at all with activation level. Thus, there appears to be a spectrum of activation dependence, with fast skeletal fibers showing the most, cardiac muscle showing the least, and soleus fibers falling in between. The finding that slow skeletal fibers show intermediate behavior is interesting in light of the fact that soleus fibers contain both the cardiac isoform of TnC (Wilkinson, 1980) and the cardiac myosin isoform (Lompre et al., 1984), and suggests that there is some further difference between cardiac and slow skeletal muscle that is responsible for the difference in the activation dependence of cross-bridge kinetics.

CONCLUSION

Using a segment length feedback system, it was possible to study the isometric force redevelopment kinetics in skinned cardiac trabeculae. By employing two different protocols to detach the cycling cross-bridges at a number of different activation levels, it was shown that the force redevelopment rate constant, k_{tr}, either did not vary or decreased slightly with activation level. Similar results were found when sarcomere length control was used at submaximum activation levels. These findings are consistent with results from intact cardiac muscle, but contrast with results from skinned slow and fast skeletal fibers. This lack of activation dependence of k_{tr} suggests that in mammalian cardiac muscle Ca^{2+} modulates the number of actomyosin interactions and not the kinetics of transitions within the cross-bridge cycle.

The authors would like to thank Martha Mathiason for computer programming assistance and Don Anderson for electronics hardware support.

This study was supported by National Institutes of Health grants HL-31962, HL-07403, and HL-52558.

REFERENCES

Allen, D. G., and J. C. Kentish. 1988. Calcium concentration in the myoplasm of skinned ferret ventricular muscle following changes in muscle length. *J. Physiol.* 407:489–503.

Araujo, A., R. L. Moss, and J. W. Walker. 1993. Tension transients in rat cardiac myocytes initiated by photolysis of caged Ca^{2+}. *Biophys. J.* 64:A254.

Araujo, A., and J. W. Walker. 1994. Kinetics of tension development in skinned cardiac myocytes measured by photorelease of Ca^{2+}. *Am. J. Physiol.* 267:H1643–H1653.

Backx, P. H., and H. E. D. J. ter Keurs. 1993. Fluorescent properties of rat cardiac trabeculae microinjected with fura-2 salt. *Am. J. Physiol.* 264: H1098–H1110.

Barsotti, R. J., H. Martin, J. H. Kaplan, and G. C. R. Ellis-Davies. 1994. Activation of skinned cardiac muscle by laser photolysis of nitrophenyl-EGTA. *Biophys. J.* 66:A5.

Brenner, B. 1988. Effect of Ca^{2+} on cross-bridge turnover kinetics in skinned single rabbit psoas fibers: implications for regulation of muscle contraction. *Proc. Natl. Acad. Sci. USA.* 85:3265–3269.

Brenner, B., and E. Eisenberg. 1986. Rate of force generation in muscle: correlation with actomyosin ATPase activity in solution. *Proc. Natl. Acad. Sci. USA.* 83:3542–3546.

Burton, K. 1991. Rapid tension recovery in response to shortening steps following a cycle of ramp shortening and large restretch in skinned rabbit psoas fibers. *Biophys. J.* 59:35a.

Caceci, M. S., and W. P. Cacheris. 1984. Fitting curves to data: the Simplex algorithm is the answer. *Byte.* May:340–362.

Chase, P. B., and M. J. Kushmerick. 1988. Effects of pH on contraction of rabbit fast and slow skeletal muscle fibers. *Biophys. J.* 53:935–946.

Chase, P. B., and M. J. Kushmerick. 1995. The effects of physiological ADP concentrations on contraction of single skinned fibers from rabbit fast and slow muscles. *Am. J. Physiol.* 286:C480–C489.

Chase, P. B., D. A. Martyn, and J. D. Hannon. 1994. Isometric force redevelopment of skinned muscle fibers from rabbit activated with and without Ca^{2+}. *Biophys J.* 67:1994–2001.

Eisenberg, B. R. 1983. Quantitative ultrastructure of mammalian skeletal muscle. *In* Handbook of Physiology. Section 10: Skeletal Muscle. L. D. Peachey, editor. American Physiological Society, Bethesda, MD. 73–112.

Goldman, Y. E., and R. M. Simmons. 1984. Control of sarcomere length in skinned muscle fibres of *Rana temporaria* during mechanical transients. *J. Physiol.* 350:497–518.

Hancock, W. O., L. L. Huntsman, D. A. Martyn, and A. M. Gordon. 1994. Isometric force kinetics are unaffected by Ca^{2+} in skinned rat ventricular myocardium. *Biophys. J.* 66:A404.

Hancock, W. O., D. A. Martyn, and L. L. Huntsman. 1993. Ca^{2+} and segment length dependence of isometric force kinetics in intact ferret cardiac muscle. *Circ. Res.* 73:603–611.

Hoh, J. F. Y., G. H. Rossmanith, L. J. Kwan, and A. M. Hamilton. 1988. Adrenaline increases the rate of cycling of crossbridges in rat cardiac muscle as measured by pseudo-random binary noise-modulated perturbation analysis. *Circ. Res.* 62:452–461.

Huntsman, L. L., J. F. Rondinone, and D. A. Martyn. 1983. Force-length relations in cardiac muscle segments. *Am. J. Physiol.* 244:H701–H707.

Huxley, A. F., and R. M. Simmons. 1973. Mechanical transients and the origin of muscular force. *Cold Spring Harb. Symp. Quant. Biol.* 37: 669–680.

Huxley, H. E. 1973. Structural changes in the actin- and myosin-containing filaments during contraction. *Cold Spring Harb. Symp. Quant. Biol.* 37:361–376.

Kentish, J. C. 1986. The effects of inorganic phosphate and creatine phosphate on force production in skinned muscles from rat ventricle. *J. Physiol.* 370:585–604.

Kentish, J. C., and G. J. M. Stienen. 1994. Differential effects of length on maximum force production and myofibrillar ATPase activity in rat skinned cardiac muscle. *J. Physiol.* 475:175–184.

Kentish, J. C., H. E. D. J. ter Keurs, L. Ricciardi, J. J. Bucx, and M. I. Noble. 1986. Comparison between the sarcomere length-force relations of intact and skinned trabeculae from rat right ventricle. Influence of calcium concentrations on these relations. *Circ. Res.* 58:755–768.

Kress, M., H. E. Huxley, and A. R. Faruqi. 1986. Structural changes during activation of frog muscle studied by time-resolved X-ray diffraction. *J. Mol. Biol.* 188:325–342.

Lehman, W., R. Craig, and P. Vibert. 1994. Ca^{2+}-induced tropomyosin movement in *Limulus* thin filaments revealed by three-dimensional reconstruction. *Nature.* 368:65–67.

Lompre, A.-M., B. Nadal-Ginard, and V. Mahdavi. 1984. Expression of the cardiac ventricular α- and β-myosin heavy chain genes is developmentally and hormonally regulated. *J. Biol. Chem.* 259:6437–6446.

Martyn, D. A., and A. M. Gordon. 1988. Length and myofilament spacing-dependent changes in calcium sensitivity of skeletal fibres: effects of pH and ionic strength. *J. Muscle Res. Cell Motil.* 9:428–45.

Martyn, D. A., and A. M. Gordon. 1992. Force and stiffness in glycerinated rabbit psoas fibers. *J. Gen. Physiol.* 99:795–816.

Metzger, J. M., M. L. Greaser, and R. L. Moss. 1989. Variations in cross-bridge attachment rate and tension with phosphorylation of myosin in mammalian skinned skeletal muscle fibers. *J. Gen. Physiol.* 93: 855–883.

Metzger, J. M., and R. L. Moss. 1990. Calcium-sensitive cross-bridge transitions in mammalian fast and slow skeletal muscle fibers. *Science.* 247:1088–1090.

Metzger, J. M., and R. L. Moss. 1991. Phosphate and the kinetics of force generation in skinned skeletal muscle fibers. *Biophys. J.* 59:418a.

Millar, N. C., and E. Homsher. 1990. The effect of phosphate and calcium on force generation in glycerinated rabbit skeletal muscle fibers: a steady-state and transient kinetic study. *J. Biol. Chem.* 265: 20234–20240.

Parry, D. A., and J. M. Squire. 1973. Structural role of tropomyosin in muscle regulation: analysis of the x-ray diffraction patterns from relaxed and contracting muscles. *J. Mol. Biol.* 75:33–55.

Rossmanith, G. H., J. F. Y. Hoh, A. Kirman, and L. J. Kwan. 1986. Influence of V1 and V3 isomyosins on the mechanical behaviour of rat papillary muscle as studied by pseudo-random binary noise modulated length perturbations. *J. Muscle Res. Cell Motil.* 7:307–319.

Shibata, T., W. C. Hunter, A. Yang, and K. Sagawa. 1987. Dynamic stiffness measured in central segment of excised rabbit papillary muscles during barium contracture. *Circ. Res.* 60:756–769.

Sweeney, H. L., and J. T. Stull. 1990. Alteration of cross-bridge kinetics by myosin light chain phosphorylation in rabbit skeletal muscle: implications for regulation of actin-myosin interaction. *Proc. Natl. Acad. Sci. USA.* 87:414–418.

VanBuren, P., D. E. Harris, N. R. Alpert, and D. M. Warshaw. 1995. Cardiac V1 and V3 myosins differ in their hydrolytic and mechanical activities in vitro. *Circ. Res.* 77:439–444.

Wilkinson, J. M. 1980. Troponin C from rabbit slow skeletal and cardiac muscle is the product of a single gene. *Eur. J. Biochem.* 103:179–188.

Wolff, M. R., K. S. McDonald, and R. L. Moss. 1995. Rate of tension development in cardiac muscle varies with level of activator calcium. *Circ. Res.* 76:154–60.